Submission is intended as Short Report

Novel origin of lamin-derived cytoplasmic intermediate filaments in tardigrades

Lars Hering[1,2,†,*], Jamal-Eddine Bouameur[3,†], Julian Reichelt[1,†], Thomas M. Magin[3] & Georg Mayer[1,2,*]

[1]Department of Zoology, Institute of Biology, University of Kassel, Heinrich-Plett-Str. 40, D-34132 Kassel, Germany

[2]Animal Evolution and Development, Institute of Biology, University of Leipzig, Talstr. 33, D-04103 Leipzig, Germany

[3]Institute of Biology and Translational Center for Regenerative Medicine, University of Leipzig, D-04103 Leipzig, Germany

[*]For correspondence: Georg Mayer (georg.mayer@uni-kassel.de), Lars Hering (lars.hering@uni-kassel.de)

[†]These authors contributed equally to this work.

Abstract

Intermediate filament (IF) proteins, including nuclear lamins and cytoplasmic IF proteins, are essential cytoskeletal components of bilaterian cells. Despite their important role in protecting tissues against mechanical force, no cytoplasmic IF proteins have been convincingly identified in arthropods. Here we show that the ancestral cytoplasmic IF protein gene was lost in the entire panarthropod (onychophoran + tardigrade + arthropod) rather than arthropod lineage and that nuclear, lamin-derived proteins instead acquired new cytoplasmic roles at least three times independently in collembolans, copepods, and tardigrades. Transcriptomic and genomic data revealed three IF protein genes in the tardigrade *Hypsibius dujardini*, one of which (cytotardin) occurs exclusively in the cytoplasm of epidermal and foregut epithelia, where it forms belt-like filaments around each epithelial cell. These results suggest that a lamin derivative has been co-opted to enhance tissue stability in tardigrades, a function otherwise served by cytoplasmic IF proteins in all other bilaterians.

Introduction

Tardigrades, also known as water bears, are microscopic invertebrates that live in marine, freshwater and semi-aquatic/limno-terrestrial environments [1, 2] (Figure 1). Although tardigrades have become renowned for their ability to survive extreme conditions [3, 4], including exposure to space [5, 6], only little is known about the actual mechanisms that allow their cells to resist severe mechanical stress caused by desiccation and freezing [3, 4, 7-9]. The integrity and plasticity of tardigrade tissues might be achieved by specialised cytoskeletal components, such as IF proteins, which are known to be essential for stress resilience of cells [10-12]. While lamins, a group of IF proteins found in the nucleus, occur in most eukaryotes, including social amoebae [13] and all metazoans [14], cytoplasmic IF proteins are thought to have evolved from an ancestral lamin gene by duplication in the bilaterian lineage [15, 16]. Genomic and biochemical studies have revealed that the cytoplasmic IF proteins are present in all bilaterian taxa excluding arthropods [17-19] (but see a contradictory report [20] of a putative cytoplasmic IF protein in a collembolan). The apparent loss of cytoplasmic IF proteins in the arthropod lineage might correlate with the acquisition of an exoskeleton [16, 18, 19], which provides mechanical support to the arthropod skin. However, this hypothesis has never been tested, as it is unknown whether or not onychophorans and tardigrades, the soft-bodied relatives of arthropods, possess cytoplasmic IF proteins.

Results and Discussion

To clarify whether or not onychophorans and tardigrades possess cytoplasmic IF proteins, we analysed Illumina-sequenced transcriptomes of five distantly related onychophoran species and the freshwater tardigrade *H. dujardini*. Although this model tardigrade [21, 22] shows only a limited ability to tolerate desiccation (anhydrobiosis), it clearly survives immediate freezing (cryobiosis; see video 1). Our analyses revealed only one putative IF protein transcript in each of the five onychophoran species but three in *H. dujardini*. Additional screening of the recently sequenced genome [23, 24] of *H. dujardini* confirms that the identified transcripts correspond to the three potential IF protein-coding genes of this species. According to sequence comparisons with well-characterized IF proteins from humans and the nematode *Caenorhabditis elegans*, all corresponding proteins of the three identified genes share a similar α-helical rod domain organization with three coiled coil-forming segments (coil 1A, coil 1B, coil 2; Figure 2A,B and Figure 2—figure supplement 1 and 2) [review 25]. This, in conjunction with the highly conserved intermediate filament consensus motifs [review 26] at the beginning and end of the rod domain of all three tardigrade proteins, classify them as intermediate filament proteins. The three tardigrade IF proteins further possess 42 residues in the coil 1B (Figure 2B and Figure 2—figure supplement 1) — a feature that is shared between all eukaryote lamins and protostome cytoplasmic IF proteins but that must have been deleted from the ancestral cytoplasmic IF protein gene in chordates [10, 27]. In contrast to the similar organization of the rod domain, the flanking sequences vary between all three tardigrade IF proteins. One of them, which we

named lamin-2, possesses all major regions known from other eukaryote lamins [10, 14, 28], including the nuclear localization signal (NLS) — which generally mediates the import of proteins into the nucleus [29] — the lamin-tail domain (LTD), and the carboxy-terminal CaaX motif (Figure 2A,B). In contrast, the second tardigrade IF protein (named lamin-1) lacks the CaaX box, whereas the third IF protein from *H. dujardini* is missing all three motifs, including the NLS, indicating this protein may instead localize in the cytoplasm rather than the nuclear lamina of *H. dujardini* cells. Since the structure of the latter resembles the domain composition of known bilaterian cytoplasmic IF proteins (Figure 2—figure supplement 1 and 2) we consequently named it cytotardin.

To firmly place the onychophoran and tardigrade IF homologs on the evolutionary tree, we reconstructed the phylogeny of broadly sampled metazoan lamin and cytoplasmic IF protein genes. In our phylogenetic analyses, all identified tardigrade and onychophoran sequences cluster within the bilaterian lamin clade, whereas none of them groups with cytoplasmic IF protein-coding genes (Figure 3 and Figure 3—figure supplement 1 and 2). Surprisingly, the three identified IF sequences of *H. dujardini*, together with two sequences from *Milnesium tardigradum*, form a strongly supported monophyletic clade of tardigrade lamins (GTR+G: Bootstrap support BS=77, LG+G: BS=80) in our analyses (Figure 3 and Figure 3—figure supplement 1 and 2). This implies that there were at least two duplication events in the tardigrade lineage that gave rise to *lamin-1*, *lamin-2* and *cytotardin* genes — consequently characterizing the tardigrade IFs (including cytotardin), for example, as co-orthologous to nematode lamins rather than orthologous to

105 nematode cytoplasmic IFs (Figure 3 and Figure 3—figure supplement 1 and 2).
106 Our results further show that the isomin sequence of the collembolan
107 *Isotomurus maculatus* does in fact cluster with other identified collembolan
108 transcripts (GTR+G: BS=74, LG+G: BS=70) within the clade of arthropod
109 lamins (Figure 3 and Figure 3—figure supplement 1 and 2); it had previously
110 been interpreted [20] as closely related to cytoplasmic IF proteins of nematodes
111 and therefore as an ortholog of the bilaterian cytoplasmic IF proteins, likely due
112 to the narrower dataset used for their phylogenetic analysis. These results
113 clearly challenge the identity of isomin as a member of the bilaterian
114 cytoplasmic IF protein clade [20] and suggest that orthologs of genes encoding
115 these proteins are entirely missing in arthropods, at least in those with known
116 genomic sequences. In fact, besides the putative IF proteins from chelicerates,
117 crustaceans and hexapods obtained from publicly available databases (e.g.
118 GenBank), our transcriptomic and genomic analyses, which included screening
119 of the genome of the centipede *Strigamia maritima* [30], the water flea *Daphnia*
120 *pulex* [31], and more than 70 transcriptomes from hexapod species sequenced
121 as part of the 1KITE project [32], strongly suggest that these genes were
122 already lost in the panarthropod lineage, since all of these panarthropod IF
123 proteins cluster within a well-supported monophyletic clade of bilaterian lamins
124 (GTR+G: BS=84, LG+G: BS=76; Figure 3—figure supplement 1 and 2). In this
125 respect, even if the metazoan lamins are polyphyletic, as recently proposed by
126 Kollmar [33] based on the finding of putative nematocilin homologs in Bilateria,
127 our results favour the tardigrade, copepod, and collembolan IF proteins as

128 members of the bilaterian lamins rather than the bilaterian cytoplasmic IFs or
129 nematocilins (Figure 3—figure supplement 1 and 2).

130 To determine their subcellular localization and organization, we generated
131 antisera against the three IF proteins of *H. dujardini* and confirmed their
132 specificity (see Figure 4—figure supplement 1 and Figure 5—figure supplement
133 1). Immunolocalization of lamin-1, lamin-2 and cytotardin proteins in whole-
134 mount preparations and cryosectioned specimens, in conjunction with confocal
135 laser-scanning microscopy, revealed a highly specific subcellular distribution
136 and tissue-restricted expression of these proteins in *H. dujardini*. As predicted,
137 lamin-1 and lamin-2 proteins both display a typical, lamin-like distribution within
138 all nuclei (Figure 4A–D and Figure 4—figure supplement 2). While lamin-1 is
139 localised throughout the nucleoplasm, lamin-2 is restricted to the nuclear
140 periphery (Figure 4B), although there is a small overlap region between these
141 two proteins (Figure 4C). The intranuclear distribution of lamin-1 corresponds to
142 its lack of the CaaX motif, which is responsible for the association of lamins with
143 the nuclear envelope [34]. In contrast to the two lamins, cytotardin of *H.*
144 *dujardini* is not localised within the nucleus, but in the peripheral cytoplasm of
145 all epidermal and foregut cells, where it appears to be closely associated or
146 aligned with the plasma membrane (Figure 4E–G and Figure 4—figure
147 supplement 3 and Figure 6—figure supplement 1). In this setting, it encircles the
148 apical regions of the cells in a belt-like, filamentous array (Figure 4E–G and
149 Figure 4—figure supplement 3).

In order to investigate the filament-forming capacity of cytotardin, we transiently transfected human mammary epithelial MCF-7 cells with a corresponding cDNA (Figure 5A–F and Figure 5—figure supplement 1). Immunofluorescence analysis using cytotardin antibody revealed that this protein is located exclusively in the cytoplasm of transfected MCF-7 cells, where it forms both short filaments and extensive cytoskeletal networks which most likely are homopolymeric (Figure 5A–F). Notably, some of the cytotardin arrays display cage-like perinuclear structures, while others are located in the periphery close to the cell membrane (Figure 5E,F). Double labelling for cytotardin and desmoplakin, a desmosomal protein mediating membrane attachment of mammalian IF proteins [35], shows that cytotardin occurs close to desmosomes but is not co-localised with desmoplakin (Figure 5C,D). To examine whether this arrangement was mediated by interactions between cytotardin and keratins endogenously expressed in MCF-7 cells, we double-labelled the transfectants for cytotardin and keratin-8. Our data show that these two proteins are not co-localised and that the endogenous keratin networks are displaced in cells with dense cytotardin arrays (Figure 5E,F). These findings strongly support an intrinsic ability of the cytotardin protein of *H. dujardini* to both form homopolymeric filaments and cytoplasmic networks — both properties that are functionally analogous to mammalian cytoplasmic IFs [36].

Our data on tissue-specific distribution of cytotardin in *H. dujardini* further show that its belt-like arrays are confined to the ectodermal epithelia, including the epidermis, buccal tube, pharynx, and oesophagus (Figures 4E–G and 6A,B and Figure 4—figure supplement 3 and Figure 6—figure supplement 1). Thus,

the entire tardigrade body is ensheathed by a grid of belt-like filaments formed by the cytotardin protein, which retain their integrity even in contracted specimens (Figure 4E–G and Figure 4—figure supplement 3 and Figure 6—figure supplement 1). The most prominent anti-cytotardin immunoreactivity is found in areas exposed to considerable physical stress in living specimens, including the bases of claws and the stylet apparatus (Figures 4F,G and 6B and Figure 4—figure supplement 3 and Figure 6—figure supplement 1). We therefore anticipate that much of the resistance of the tardigrade body to extreme conditions, such as cryobiosis [7, 37], might be attributable to the dense, fibre-like cytotardin meshwork. The belt-like structures encircling each epidermal cell might help to resist the shearing forces that arise during freezing and thawing cycles, whereas the dense meshwork at the basis of each claw and around the stylets might provide the tissue stability necessary for locomotion and feeding.

Together, our data demonstrate that cytotardin of *H. dujardini* is a cytoplasmic IF protein, predominantly expressed in ectodermal epithelia, that has evolved independently from the cytoplasmic IF proteins of other bilaterians by gene duplication and subsequent neofunctionalization (Figure 6C). This process was most likely triggered by an initial loss of the CaaX motif and nuclear localization signal from the ancestral *cytotardin* gene in the tardigrade lineage. Expression of the cytotardin protein in tissues that are subject to mechanical stress might have served as a pre-adaptation for the ability of tardigrades to survive extreme environmental conditions. Similar duplication and neofunctionalization events might have occurred in the collembolan and

198 copepod lineages, as our findings demonstrate that these two taxa also show
199 duplicated lamins that have lost their nuclear localization signals (Figures 3 and
200 6C and Figure 3—figure supplement 1 and 2). While isomin might stabilize the
201 intestinal epithelial cells in collembolans [20], the localization and function of the
202 putative lamin-derived cytoplasmic IF protein in copepods has yet to be
203 clarified.

204

205 ## Materials and Methods

206 ### Culturing of specimens, transcriptomics, genomics and phylogenetic
207 ### analyses

208 Specimens of *Hypsibius dujardini* (DOYÈRE, 1840) were purchased from Sciento
209 (Manchester, UK) and cultured as described by Mayer, et al. [38]. The Illumina-
210 sequenced transcriptomes of *H. dujardini* and five onychophoran species from
211 Hering, et al. [39] and Hering and Mayer [40] were screened for expressed
212 intermediate filament genes, including lamins, by BLAST searches [41] with
213 known metazoan lamins and cytoplasmic IF genes as bait sequences. Three
214 putative IF protein genes from *H. dujardini* and one from each of the
215 onychophoran species studied were verified afterwards by reciprocal BLAST
216 searches against the nr database of GenBank
217 (http://blast.ncbi.nlm.nih.gov/Blast.cgi). In addition, BLAST searches of the
218 putative tardigrade intermediate filament genes in the genome of *H. dujardini*
219 (http://badger.bio.ed.ac.uk/H_dujardini/) yielded nearly identical sequences as
220 obtained in our transcriptomic data, although the automatically predicted
221 transcripts from the genome seem to be erroneous as previously reported by
222 Hering and Mayer [40] and had to be corrected manually. Furthermore, publicly
223 available resources and databases (nr, TSA and EST databases of GenBank,
224 Compagen [42]) as well as the genome of the centipede *Strigamia maritima*
225 [30], the water flea *Daphnia pulex* [31], and more than 70 transcriptomes from
226 hexapod species sequenced as part of the 1KITE project [32] were
227 comprehensively screened for putative eukaryotic intermediate filament genes.
228 In total, 447 eukaryotic lamin and cytoplasmic IF genes were manually curated

229 and selected for further analyses. Each of the sequences was verified by
230 screening for the presence of a coiled-coil-forming domain (Pfam PF00038), a
231 typical feature of intermediate filament proteins, and the presence or absence of
232 a lamin tail domain (LTD; Pfam PF00932, SCOP d1ifra_, PDB
233 2lll/2kpw/1ufg/1ivt) using the webserver of Pfam 27.0 [43] and SMART [44, 45],
234 respectively. In addition, the occurrence of a nuclear localization signal (NLS
235 motif) was predicted for all sequences by using the webserver of NucPred [46]
236 and cNLS Mapper [47] (cut-off score = 2.0). The protein structures (α-helices
237 and β-sheets) were predicted for the tardigrade lamin-1, lamin-2 and cytotardin
238 using Jpred3 and JNetPRED [48]. For phylogenetic analyses, the rod domains
239 of all sequences were aligned using the Mafft online version v7.245 [49] with
240 the most accurate option L-INS-i and default parameters. To remove
241 homoplastic and random-like positions, the alignment was afterwards masked
242 with the software Noisy rel. 1.15.12 [50] (-cutoff=0.8, -seqtype=P, -
243 shuffles=20,000). Two Maximum likelihood analyses were conducted with the
244 Pthreads version of RAxML v8.1.15 [51]. For each run, the best tree was
245 obtained from 10 independent inferences and GAMMA correction of the final
246 tree under either the empirical LG substitution model or a dataset-specific GTR
247 substitution matrix. The LG model was automatically selected by RAxML
248 (PROTGAMMAAUTO option) as best-fitting substitution model, which is in line
249 with the best-fitting model obtained with ProtTest v3.4.1 [52] (LG+G) according
250 to the Akaike information criterion [53] (AIC), Bayesian Information Criterion [54]
251 (BIC), corrected AIC [55, 56], and Decision Theory Criterion [57] (DT). Notably,
252 the analysis using the dataset-specific GTR+G model yielded a better log

likelihood score (−174,216.74) for the best tree than using the best obtained empirical model LG+G (−178,092.26). Bootstrap support values for both trees were calculated using the rapid bootstrapping algorithm implemented in RAxML from 1,000 pseudoreplicates. The protein domain structures of the sequences analysed were mapped on the trees using iTol v2 [58].

Cloning

Total RNA from several hundred specimens of *H. dujardini* was extracted and purified using TRIzol® Reagent (Life Technologies) and RNeasy MinElute Cleanup Kit (Qiagen) according to the manufacturers' protocols. First strand cDNA synthesis was performed using random hexamer primer and SuperScript® II Reverse Transcriptase (Life Technologies) and afterwards used as template for amplification of the whole coding sequence (CDS) of *lamin-1*, *lamin-2* and *cytotardin* using gene specific primers. The *cytotardin* specific primers contained restriction sites that were required for subsequent cloning into bacterial or mammalian expression vectors (see Figure 5—figure supplement 2). The amplicons of *lamin-1* and *lamin-2* were cloned into the pGEM®-T Vector System (Promega) to generate the plasmids pGEM-T-lamin-1 and pGEM-T-lamin-2. *Cytotardin* CDS was cloned into expression vectors pET15b (Novagen), pcDNA™3.1/Zeo $^{(+)}$ (Life Technologies) and pEGFP-C3 (Clontech) to generate the following plasmids: pET15b-cytotardin, pcDNA3-cytotardin, pcDNA3-HA-cytotardin and pEGFP-cytotardin. All PCR-amplified constructs were verified by Sanger sequencing and have been deposited in

GenBank (http://www.ncbi.nlm.nih.gov/genbank) under accession numbers KU295460–KU295467.

Antibody generation

Polyclonal antibodies against HPLC-purified synthetic peptides (C-terminal) of lamin-1, lamin-2 and cytotardin of *H. dujardini* were newly generated, following coupling to KLH (key limpet hemocyanin) (Peptide Specialty Laboratories GmbH, Heidelberg, Germany). Anti-lamin-1 (antigen: SNLDIHNDSVRDSPRSAG-C) and anti-cytotardin (antigen: EQKITETFKASGRVGPRTDW-C) were purified from sera of immunised guinea pigs and anti-lamin-2 (antigen: REMTQSSTRDDSYLGPSGLPKR-C) from the serum of immunised rabbits (Peptide Specialty Laboratories GmbH).

Immunolocalization in whole-mount preparations and cryosections

For cryosectioning, specimens of *H. dujardini* were concentrated by filtering the culture medium through a polyamide mesh (pore size: 30 µm). The concentrated specimens were transferred into an embedding medium for cryosectioning (Tissue-Tek® O.C.T™ Compound, Sakura Finetek, USA). Single drops of the medium containing the tardigrades were immediately frozen in dry ice-cooled 2-methylbutane. The frozen drops were cryosectioned into 5 µm thick sections. The sections were attached to SuperFrost® Plus slides (Menzel, Braunschweig, Germany), then dried at room temperature and stored at −80 °C. The ice-cooled cryosections were fixed on slides with a 4 % solution of formalin (FA) freshly prepared from paraformaldehyde in phosphate-buffered saline

(PBS; 0.1 M, pH 7.4) for 15 minutes. The sections were then shortly washed with an ammonium chloride solution (50 mM in PBS) and rinsed in Tris-buffered saline (TBS; 0.01 M, pH 7.6) two times for three minutes each. The anti-lamin-1 serum was applied to cryosections at a concentration of 1.9 µg/mL in TBS containing 1 % bovine serum albumin (BSA). Equally applied were the anti-lamin-2 serum with a concentration of 1.8 µg/mL and the anti-cytotardin serum with a concentration of 2.1 µg/mL. The incubation with the primary antibody solution was performed at room temperature for one hour. After two 3-minute washing steps in TBS, a secondary antibody, either donkey anti-guinea pig Alexa Fluor® 488 (Jackson ImmunoResearch Laboratories, Hamburg; 3 µg/mL in TBS with 1 % BSA) for anti-lamin-1 and anti-cytotardin or goat anti-rabbit Alexa Fluor® 568 (Molecular Probes; 4 µg/mL in TBS with 1 % BSA) for anti-lamin-2, was applied at room temperature for one hour. The sections were then washed in TBS two times for three minutes and shortly rinsed with distilled water and afterwards with ethanol (100 %).

For whole-mount immunocytochemistry, specimens were first concentrated as described above and then pipetted into a 1 mL Eppendorf tube. After carefully removing excess water, the specimens were flash-frozen by placing each tube on dry ice. Frozen specimens were fixed immediately by applying a 4 % solution of formaldehyde (FA) in PBS with 1 % dimethyl sulfoxide (DMSO). The fixative was applied at room temperature overnight. The whole-mounts were then washed in PBS two times for 10 minutes, two times for 30 minutes and two times for an hour. The specimens were cleared by dehydration in an ascending ethanol series (70 %, 90 %, 95 %, 100 %, 100 %),

applying xylene as a clearing agent two times for three minutes and rehydration in a descending ethanol series (100 %, 100 %, 90 %, 70 %, 50 %). The whole-mount preparations were then washed at 37 °C in PBS two times for 10 minutes. A mixture of Collagenase/Dispase (Roche Diagnostics, Mannheim; each 1 mg/mL) and hyaluronidase (Sigma-Aldrich, Munich; 1 mg/mL) diluted in PBS was applied at 37 °C for 10 minutes. After the incubation with enzymes, a 15-minute post-fixation with 4 % FA in PBS followed at room temperature. The specimens were washed in an ammonium chloride solution (50 mM) two times for 15 minutes, afterwards in PBS with 1 % Triton X-100 (Sigma-Aldrich) two times for 10 minutes, two times for 30 minutes, once for an hour, overnight and then two times for 1 minute. The whole-mount preparations were incubated in a blocking solution containing 10 % normal goat serum (NGS; Sigma-Aldrich), 1 % Triton X-100 and 1 % DMSO in PBS at room temperature for one hour. The anti-cytotardin serum with a concentration of 4.2 µg/mL in PBS with 1 % NGS, 1 % DMSO and 0.02 % sodium azide was applied at room temperature for three days. After washing in PBS with 1 % Triton X-100 and 1 % DMSO three times for five minutes, two times for 15 minutes, four times for two hours, overnight and two times for 15 minutes a secondary antibody (donkey anti-guinea pig Alexa Fluor 488) with a concentration of 3 µg/mL in PBS with 1 % NGS, 1 % DMSO and 0.02 % sodium azide was applied at room temperature for three days. Finally the specimens were washed in PBS with 1 % Triton X-100 and 1 % DMSO three times for five minutes, three times for 15 minutes and two times for one hour and afterwards in PBS (without Triton X-100 and DMSO) four times for 15 minutes.

Either DAPI (1 µg/mL; Carl Roth, Karlsruhe), SYBR Green I (diluted 1:10,000; Molecular Probes, Darmstadt), propidium iodide (0.5 µg/mL; Carl Roth) or TO-PRO-3 iodide (diluted 1:1,000; Molecular Probes) were used as nuclear counterstain markers. Each of these fluorescent dyes was simply added to the solution containing the secondary antibody. Cryosections and whole-mount preparations were mounted in Prolong Gold antifade reagent (Molecular Probes). The whole-mount preparations were mounted between two cover slips using petrolatum at all corners as spacer. All slides and cover slips were sealed at the edges with transparent nail polish for long time storage. Specimens were analysed with the confocal laser-scanning microscopes Zeiss LSM 780 (Carl Zeiss Microscopy, Göttingen, Germany) and Leica TCS STED (Leica Microsystems CMS, Wetzlar, Germany).

Recombinant protein expression of cytotardin in bacteria

Escherichia coli BL21 (DE3) were transformed with pET15b or pET15b-cytotardin vectors. Expression of recombinant protein was induced with 0.1 mM IPTG for 3 hours in *Luria Bertani* (LB) medium. Bacterial suspensions were centrifuged at 3,000 g for 10 min at 4 °C. Bacterial pellets were then washed twice in PBS and lysed in 5X Laemmli buffer (Volume in µL = OD600/10xVolume of culture in mL) containing protease inhibitor (Thermo Scientific, #78439), heated at 95 °C for 10 min, briefly sonicated and heated again. Lysate of cells transformed with pET15b-cytotardin was diluted at 1:50. Recombinant cytotardin protein expression was first assessed by Coomassie blue stained SDS-PAGE and further by Western blotting.

Transfection and immunolabelling of cytotardin in MCF-7 cell culture

Cells from the human cell line MCF-7 (ATCC® HTB-22™) were cultured in Dulbecco's modified Eagle's medium (DMEM, GE Healthcare) supplemented with 10 % foetal bovine serum (FBS, GE Healthcare), 100 U/mL penicillin, and 100 µg/mL streptomycin. Cells were transfected with pcDNA-cytotardin, pcDNA-HA-cytotardin, pEGFP-cytotardin and the corresponding empty vectors using Xfect Transfection reagent (Clontech) according to the manufacturer's protocol. For immunofluorescence microscopy, cells were grown on glass slides and fixed 24 hours after transfection. MCF-7 cells were washed twice with PBS and fixed either in methanol or in 4 % FA freshly prepared from paraformaldehyde in PBS. For methanol fixation, cells grown on a coverslip were put in ice-cold methanol for 10 min, acetone for 1 min and dried at RT for 30 min. For FA fixation, cells were put in a 4 % FA solution in PBS for 15 min at RT. After fixation, cells were washed in PBS and used for immunolabelling. FA-fixed cells were first permeabilised in PBS 0.1 % Triton X-100 for 5 min and blocked in PBS 5 % bovine serum albumin for 30 min. Methanol- and FA-fixed cells were then incubated overnight at 4 °C with primary antibody solutions, washed 3 times, incubated in secondary antibodies + DAPI (Sigma) solution for 1 h, washed 2× in PBS, 1× in water, 1× in 100 % ethanol, dried for 30 min and mounted in mounting medium (Dianova). Primary antibodies were used at the following dilutions: guinea pig anti-cytotardin, 1:1,000; mouse anti-desmoplakin (11-5F), 1:150; mouse anti-keratin-8 (Ks 8.7), 1:100; mouse anti-HA-tag (Covance MMS-101P), 1:100. Images were taken using a confocal microscope

(LSM 780; Carl Zeiss Microscopy GmbH) with 63×/1.46 NA oil immersion objective and Z-stack images were assembled by "Maximum Intensity Projection" of the ZEN 2012 software (Carl Zeiss).

Western blotting and specificity tests

Western blots were performed either on lysates of transfected MCF-7 cells or multiple specimens of *H. dujardini*. Transfected MCF-7 cells grown in 10 cm^2 dishes were lysed in 200 µL 5× Laemmli sample buffer and boiled for 10 min at 98 °C and briefly centrifuged prior to use. Concentrated specimens of *H. dujardini* were lysed in 800 µL 5× Laemmli buffer containing protease inhibitor, boiled for 10 min, sonicated and boiled again for 10 min. SDS-PAGE and Western blotting were performed as described previously [59]. Primary antibodies, diluted in Tris-buffered saline containing 0.05 % Tween 20 (AppliChem, A4974), were used at the following concentrations: anti-lamin-1, 1:10,000; anti-lamin-2, 1:5,000; anti-cytotardin, 1:10,000, anti-HA tag (Covance MMS-101P), 1:1,000 and anti-GFP (Santa Cruz Biotechnology, sc-5385), 1:1,000. Anti-lamin-1 and anti-lamin-2 antibodies were only tested in Western blots based on lysates of tardigrade specimens.

Acknowledgements

We thank Sandra Treffkorn and Vladimir Gross for help with tardigrade culture, Fanny Loschke for assistance with confocal microscopy, Susann Kauschke for the light micrograph in Figure 1, Miriam Richter and Gabi Baumbach for technical assistance with cloning and cell culture, and Vladimir Gross, Jens

Bohnekamp and Matthias Behr for critical discussions. We are grateful to members of Luca Borradori's laboratory (Bern, Switzerland) for providing the pet15b vector. This work was partially supported by the German Research Foundation (DFG; INF 268/230-1; MA1316/21-1) to T.M.M. and the Emmy Noether Programme of the DFG (Ma 4147/3-1) to G.M. The authors declare no conflicts of interests.

References

1. Kinchin, I.M. (1994). The Biology of Tardigrades, (London: Portland Press Inc.).
2. Nelson, D.R. (2002). Current status of the Tardigrada: evolution and ecology. Integr. Comp. Biol. *42*, 652–659.
3. Møbjerg, N., Halberg, K.A., Jørgensen, A., Persson, D., Bjørn, M., Ramløv, H., and Kristensen, R.M. (2011). Survival in extreme environments – on the current knowledge of adaptations in tardigrades. Acta Physiol. *202*, 409–420.
4. Ramløv, H., and Westh, P. (2001). Cryptobiosis in the eutardigrade *Adorybiotus (Richtersius) coronifer*: Tolerance to alcohols, temperature and *de novo* protein synthesis. Zool. Anz. *240*, 517–523.
5. Persson, D., Halberg, K.A., Jørgensen, A., Ricci, C., Møbjerg, N., and Kristensen, R.M. (2011). Extreme stress tolerance in tardigrades: surviving space conditions in low earth orbit. J. Zool. Syst. Evol. Res. *49 (Suppl. 1)*, 90–97.
6. Rebecchi, L., Altiero, T., Cesari, M., Bertolani, R., Rizzo, A.M., Corsetto, P.A., and Guidetti, R. (2011). Resistance of the anhydrobiotic eutardigrade *Paramacrobiotus richtersi* to space flight (LIFE–TARSE mission on FOTON-M3). J. Zool. Syst. Evol. Res. *49 (Suppl. 1)*, 98–103.
7. Wright, J.C. (2001). Cryptobiosis 300 years on from van Leuwenhoek: what have we learned about tardigrades? Zool. Anz. *240*, 563–582.
8. Tanaka, S., Tanaka, J., Miwa, Y., Horikawa, D.D., Katayama, T., Arakawa, K., Toyoda, A., Kubo, T., and Kunieda, T. (2015). Novel mitochondria-targeted heat-soluble proteins identified in the anhydrobiotic tardigrade improve osmotic tolerance of human cells. PLOS One *10*, e0118272.
9. Yamaguchi, A., Tanaka, S., Yamaguchi, S., Kuwahara, H., Takamura, C., Imajoh-Ohmi, S., Horikawa, D.D., Toyoda, A., Katayama, T., Arakawa, K., et al. (2012). Two novel heat-soluble protein families abundantly expressed in an anhydrobiotic tardigrade. PLOS One *7*, e44209.
10. Herrmann, H., Strelkov, S.V., Burkhard, P., and Aebi, U. (2009). Intermediate filaments: primary determinants of cell architecture and plasticity. J Clin Invest *119*, 1772–1783.
11. Coulombe, P.A., and Wong, P. (2004). Cytoplasmic intermediate filaments revealed as dynamic and multipurpose scaffolds. Nat Cell Biol *6*, 699–706.
12. Kim, S., and Coulombe, P.A. (2007). Intermediate filament scaffolds fulfill mechanical, organizational, and signaling functions in the cytoplasm. Genes Dev *21*, 1581–1597.
13. Krüger, A., Batsios, P., Baumann, O., Luckert, E., Schwarz, H., Stick, R., Meyer, I., and Graf, R. (2012). Characterization of NE81, the first lamin-like nucleoskeleton protein in a unicellular organism. Mol Biol Cell *23*, 360–370.
14. Dittmer, T.A., and Misteli, T. (2011). The lamin protein family. Genome Biol. *12*, 222.
15. Erber, A., Riemer, D., Hofemeister, H., Bovenschulte, M., Stick, R., Panopoulou, G., Lehrach, H., and Weber, K. (1999). Characterization of the *Hydra* lamin and its gene: A molecular phylogeny of metazoan lamins. J. Mol. Evol. *49*, 260–271.
16. Herrmann, H., and Strelkov, S.V. (2011). History and phylogeny of intermediate filaments: now in insects. BMC Biol. *9*, 16.
17. Bartnik, E., and Weber, K. (1989). Widespread occurrence of intermediate filaments in invertebrates; common principles ans aspects of diversion. Eur. J. Cell Biol. *50*, 17–33.

18. Goldstein, L.S., and Gunawardena, S. (2000). Flying through the *Drosophila* cytoskeletal genome. J Cell Biol *150*, F63–F68.
19. Erber, A., Riemer, D., Bovenschulte, M., and Weber, K. (1998). Molecular phylogeny of metazoan intermediate filament proteins. J. Mol. Evol. *47*, 751–762.
20. Mencarelli, C., Ciolfi, S., Caroti, D., Lupetti, P., and Dallai, R. (2011). Isomin: a novel cytoplasmic intermediate filament protein from an arthropod species. BMC Biol. *9*, 17.
21. Gabriel, W.N., McNuff, R., Patel, S.K., Gregory, T.R., Jeck, W.R., Jones, C.D., and Goldstein, B. (2007). The tardigrade *Hypsibius dujardini*, a new model for studying the evolution of development. Dev. Biol. *312*, 545–559.
22. Gross, V., Treffkorn, S., and Mayer, G. (2015). Tardigrada. In Evolutionary Developmental Biology of Invertebrates, A. Wanninger, ed. (Berlin: Springer).
23. Boothby, T.C., Tenlen, J.R., Smith, F.W., Wang, J.R., Patanella, K.A., Osborne Nishimura, E., Tintori, S.C., Li, Q., Jones, C.D., Yandell, M., et al. (2015). Evidence for extensive horizontal gene transfer from the draft genome of a tardigrade. Proc. Natl. Acad. Sci. U.S.A.
24. Koutsovoulos, G., Kumar, S., Laetsch, D.R., Stevens, L., Daub, J., Conlon, C., Maroon, H., Thomas, F., Aboobaker, A., and Blaxter, M. (2015). The genome of the tardigrade *Hypsibius dujardini*. bioRxiv.
25. Chernyatina, A.A., Guzenko, D., and Strelkov, S.V. (2015). Intermediate filament structure: the bottom-up approach. Curr. Opin. Cell. Biol. *32*, 65–72.
26. Herrmann, H., and Aebi, U. (2004). Intermediate filaments: molecular structure, assembly mechanism, and integration into functionally distinct intracellular scaffolds. Annu. Rev. Biochem. *73*, 749–789.
27. Peter, A., and Stick, R. (2015). Evolutionary aspects in intermediate filament proteins. Curr. Opin. Cell. Biol. *32*, 48–55.
28. Burke, B., and Stewart, C.L. (2013). The nuclear lamins: flexibility in function. Nat. Rev. Mol. Cell Biol. *14*, 13–24.
29. Mical, T.I., Luther, P.W., and Monteiro, M.J. (2004). Intracellular assembly and sorting of intermediate filament proteins: role of the 42 amino acid lamin insert. Exp Cell Res *295*, 183–193.
30. Chipman, A.D., Ferrier, D.E.K., Brena, C., Qu, J., Hughes, D.S.T., Schröder, R., Torres-Oliva, M., Znassi, N., Jiang, H., Almeida, F.C., et al. (2014). The first myriapod genome sequence reveals conservative arthropod gene content and genome organisation in the centipede *Strigamia maritima*. PLOS Biol. *12*, e1002005.
31. Colbourne, J.K., Pfrender, M.E., Gilbert, D., Thomas, W.K., Tucker, A., Oakley, T.H., Tokishita, S., Aerts, A., Arnold, G.J., Basu, M.K., et al. (2011). The ecoresponsive genome of *Daphnia pulex*. Science *331*, 555–561.
32. Misof, B., Liu, S., Meusemann, K., Peters, R.S., Donath, A., Mayer, C., Frandsen, P.B., Ware, J., Flouri, T., Beutel, R.G., et al. (2014). Phylogenomics resolves the timing and pattern of insect evolution. Science *346*, 763–767.
33. Kollmar, M. (2015). Polyphyly of nuclear lamin genes indicates an early eukaryotic origin of the metazoan-type intermediate filament proteins. Scientific Reports *5*, 10652.
34. Kitten, G.T., and Nigg, E.A. (1991). The CaaX motif is required for isoprenylation, carboxyl methylation, and nuclear membrane association of lamin B2. J Cell Biol *113*, 13–23.
35. Simpson, C.L., Patel, D.M., and Green, K.J. (2011). Deconstructing the skin: cytoarchitectural determinants of epidermal morphogenesis. Nat. Rev. Mol. Cell Biol. *12*, 565–580.

36. Bohnekamp, J., Cryderman, D.E., Paululat, A., Baccam, G.C., Wallrath, L.L., and Magin, T.M. (2015). A *Drosophila* model of epidermolysis bullosa simplex. J. Invest. Dermatol.
37. Hengherr, S., Worland, M.R., Reuner, A., Brummer, F., and Schill, R.O. (2009). Freeze tolerance, supercooling points and ice formation: comparative studies on the subzero temperature survival of limno-terrestrial tardigrades. J. Exp. Biol. *212*, 802–807.
38. Mayer, G., Hering, L., Stosch, J.M., Stevenson, P.A., and Dircksen, H. (2015). Evolution of pigment-dispersing factor neuropeptides in Panarthropoda: insights from Onychophora (velvet worms) and Tardigrada (water bears). J. Comp. Neurol. *523*, 1865–1885.
39. Hering, L., Henze, M.J., Kohler, M., Kelber, A., Bleidorn, C., Leschke, M., Nickel, B., Meyer, M., Kircher, M., Sunnucks, P., et al. (2012). Opsins in Onychophora (velvet worms) suggest a single origin and subsequent diversification of visual pigments in arthropods. Mol. Biol. Evol. *29*, 3451–3458.
40. Hering, L., and Mayer, G. (2014). Analysis of the opsin repertoire in the tardigrade *Hypsibius dujardini* provides insights into the evolution of opsin genes in Panarthropoda. Genome Biol. Evol. *6*, 2380–2391.
41. Altschul, S.F., Madden, T.L., Schäffer, A.A., Zhang, J., Zhang, Z., Miller, W., and Lipman, D.J. (1997). Gapped BLAST and PSI-BLAST: a new generation of protein database search programs. Nucleic Acids Res. *25*, 3389–3402.
42. Hemmrich, G., and Bosch, T.C.G. (2008). Compagen, a comparative genomics platform for early branching metazoan animals, reveals early origins of genes regulating stem-cell differentiation. BioEssays *30*, 1010–1018.
43. Finn, R.D., Bateman, A., Clements, J., Coggill, P., Eberhardt, R.Y., Eddy, S.R., Heger, A., Hetherington, K., Holm, L., Mistry, J., et al. (2014). Pfam: the protein families database. Nucleic Acids Res. *42*, D222–D230.
44. Schultz, J., Milpetz, F., Bork, P., and Ponting, C.P. (1998). SMART, a simple modular architecture research tool: Identification of signaling domains. Proc. Natl. Acad. Sci. U.S.A. *95*, 5857–5864.
45. Letunic, I., Doerks, T., and Bork, P. (2015). SMART: recent updates, new developments and status in 2015. Nucleic Acids Res. *43*, D257–D260.
46. Brameier, M., Krings, A., and MacCallum, R.M. (2007). NucPred—Predicting nuclear localization of proteins. Bioinformatics *23*, 1159–1160.
47. Kosugi, S., Hasebe, M., Tomita, M., and Yanagawa, H. (2009). Systematic identification of cell cycle-dependent yeast nucleocytoplasmic shuttling proteins by prediction of composite motifs. Proc. Natl. Acad. Sci. U.S.A. *106*, 10171–10176.
48. Cole, C., Barber, J.D., and Barton, G.J. (2008). The Jpred 3 secondary structure prediction server. Nucleic Acids Res. *36*, W197–W201.
49. Katoh, K., and Standley, D.M. (2013). MAFFT multiple sequence alignment software version 7: improvements in performance and usability. Mol. Biol. Evol. *30*, 772–780.
50. Dress, A., Flamm, C., Fritzsch, G., Grünewald, S., Kruspe, M., Prohaska, S., and Stadler, P. (2008). Noisy: identification of problematic columns in multiple sequence alignments. Alg. Mol. Biol. *3*, 7.
51. Stamatakis, A. (2014). RAxML version 8: a tool for phylogenetic analysis and post-analysis of large phylogenies. Bioinformatics *30*, 1312–1313.
52. Darriba, D., Taboada, G.L., Doallo, R., and Posada, D. (2011). ProtTest 3: fast selection of best-fit models of protein evolution. Bioinformatics *27*, 1164–1165.
53. Akaike, H. (1974). A new look at the statistical model identification. IEEE T. Automat. Control *19*, 716–723.

54. Schwarz, G. (1978). Estimating the dimension of a model. Ann. Stat. *6*, 461–464.
55. Sugiura, N. (1978). Further analysis of the data by Akaike's information criterion and the finite corrections. Commun. Stat. Theory *7*, 13–26.
56. Hurvich, C.M., and Tsai, C.-L. (1989). Regression and time series model selection in small samples. Biometrika *76*, 297–307.
57. Minin, V., Abdo, Z., Joyce, P., and Sullivan, J. (2003). Performance-based selection of likelihood models for phylogeny estimation. Syst. Biol. *52*, 674–683.
58. Letunic, I., and Bork, P. (2011). Interactive Tree Of Life v2: online annotation and display of phylogenetic trees made easy. Nucleic Acids Res. *39*, W475–W478.
59. Löffek, S., Wöll, S., Höhfeld, J., Leube, R.E., Has, C., Bruckner-Tuderman, L., and Magin, T.M. (2010). The ubiquitin ligase CHIP/STUB1 targets mutant keratins for degradation. Hum. Mutat. *31*, 466–476.
60. McWilliam, H., Li, W., Uludag, M., Squizzato, S., Park, Y.M., Buso, N., Cowley, A.P., and Lopez, R. (2013). Analysis Tool Web Services from the EMBL-EBI. Nucleic Acids Res. *41*, W597–W600.

Figure Legends

Figure 1. Light micrograph of a specimen of the tardigrade *Hypsibius dujardini* in dorsal view. Anterior is left. Scale bar: 20 µm.

Figure 2. Structure and organization of the IF proteins of the tardigrade *Hypsibius dujardini*. (**A**) Protein sequence alignment of *H. dujardini* IF proteins with human (*Homo sapiens*) lamins A and B1. The names of *H. dujardini* IF proteins were chosen according their structural similarities to known IF proteins (lamin-1 and lamin-2: lamin-like; cytotardin: cytoplasmic IF-like; see text for details). Note the sequence similarities of the rod domains (coil 1A, L1, coil 1B, linker L12 and coil 2) and the intermediate filament consensus motifs (highlighted in red with highly conserved parts in a box) among all three proteins. The positions of rod sub-domains are placed as described for human IF proteins [review 25]. The nuclear localization signal in lamin-1, lamin-2, lamin A and lamin B1 is highlighted in green and the immunoglobulin fold (Ig fold) is marked in light orange. Note the absence of an Ig fold in cytotardin. Predictions (Jpred3, JNetPRED) of α-helices and β-sheets are indicated by red waved underlines and solid underlines, respectively. The C-terminal prenylation motif of lamins (CaaX) is marked in purple. The alignment (Clustal Omega) has been performed using Analysis Tool Web Services from the EMBL-EBI [60]. (*) indicates positions which have a single, fully conserved residue. (:) Indicates conservation between groups of strongly similar properties — scoring > 0.5 in the Gonnet PAM 250 matrix. (.) Indicates conservation between groups of weakly similar properties — scoring ≤ 0.5 in the Gonnet PAM 250 matrix. (**B**)

624 Organization of the three IF proteins of *H. dujardini*. Dark blue colour in the 1B
625 coil of the rod domain indicates six heptads that have been lost in the chordate
626 lineage of cytoplasmic intermediate filament proteins. The numbers denote the
627 amino acid positions of the beginning and end of each rod sub-domain. 1A, 1B
628 and 2, coiled-coil segments of the rod domain; CaaX, isoprenylation motif at the
629 carboxyl terminus; LTD, lamin tail domain; NLS, nuclear localization signal.
630
631 **Figure 3.** Phylogeny of the metazoan intermediate filament proteins illustrating
632 the position of the three tardigrade IF proteins (highlighted in red). The tree was
633 obtained from a Maximum likelihood analysis under a dataset-specific GTR+G
634 substitution model of 447 eukaryotic intermediate filament proteins (see Figure
635 3—figure supplement 1 for the full tree). Note that all tardigrade as well as
636 collembolan (green) and copepod IF proteins (purple) belong to the bilaterian
637 lamin clade (light blue). Hence, cytotardin and isomin are closer related to, for
638 example, nematode lamins (light brown) than to nematode cytoplasmic IF
639 proteins (dark brown), which are orthologs of the bilaterian cytoplasmic IF
640 proteins (yellow). Selected bootstrap support values are given at particular
641 nodes.
642
643 **Figure 4.** Immunofluorescence labelling of IF proteins in the tardigrade
644 *Hypsibius dujardini*. Confocal laser-scanning micrographs. (**A–D**) Triple labelling
645 of lamin-1 (green), lamin-2 (red) and DNA (cyan). Note the localization of lamin-
646 1 within the nucleoplasm and that of lamin-2 at the nuclear periphery. (**E, F**)
647 Double labelling of cytotardin (glow-mode) and DNA (cyan) on cryosections. (**E**)

Tangential section of dorsolateral body wall. Arrow points to the dorsal midline. (**F**) Cross-section of a specimen. Dorsal is up. (**G**) Whole-mount preparation of a contracted specimen in ventral view. Anterior is up. Inset shows detail of the tip of a leg. cl, claw; ep, epidermis; hd, head; lg, leg; lg1–lg4, legs 1 to 4; nu, nucleus; vs, ventral body surface. Scale bars: (**A–D**) 1 µm, (**E**) 5 µm, (**F, G**) 10 µm.

Figure 5. Immunolocalization of exogenous cytotardin in human MCF-7 epithelial cells. (**A, B**) Double labelling of cytotardin (glow-mode) and DNA (cyan). Note the cytoplasmic cytotardin filamentous network surrounding the nucleus and extensions close to cell borders. Short cytotardin filaments are aligned along the plasma membrane, different from the arrangement seen in tardigrade epithelial cells. (**C, D**) Triple labelling of cytotardin (glow-mode), desmoplakin (green) and DNA (cyan). Note that cytotardin forms a cytoplasmic filamentous network extending from the perinuclear area to the cell membrane. Note also that it is not co-localised with desmoplakin. (**E, F**) Triple labelling of cytotardin (glow-mode), keratin-8 (green) and DNA (cyan). Endogenous keratin networks have been displaced by cytotardin filaments from the perinuclear region without being disrupted (asterisk). dp, desmosomal plaque; nu, nucleus. Scale bars: (**A–F**) 10 µm.

Figure 6. Distribution of cytotardin within the cell and across the tissues in *Hypsibius dujardini* and the evolutionary history of cytoplasmic intermediate filament proteins. (**A**) Diagram of an epidermal cell of *H. dujardini* with a belt-like

672 arrangement of cytotardin. (**B**) Diagram of *H. dujardini* showing the distribution
673 of cytotardin (red), which is confined to the ectodermal tissues. (**C**) Scenario of
674 the independent origin of lamin-derived cytoplasmic intermediate filaments in
675 tardigrades, collembolans, and copepods. Note that the cytoplasmic IFs in
676 these three lineages (indicated in red, purple, and green, respectively) evolved
677 independently from the cytoplasmic IFs of other bilaterians (highlighted in
678 orange). ba, buccal apparatus; br, brain; cb, cytotardin filament belt; cg, claw
679 gland; cm, cell membrane; ep, epidermis; mi, midgut; nu, nucleus; oe,
680 oesophagus; ov, ovary; ph, pharynx.
681

Figure Supplement

Figure 2—figure supplement 1. Protein sequence alignment of *H. dujardini* cytotardin with selected human (*Homo sapiens*) cytoplasmic IF proteins. Human type I keratins K14 (epidermis) and K18 (simple epithelia) are forming IFs from obligatory heterodimers with type II keratins K5 (epidermis) and K8, respectively. The type III IF protein vimentin is able to form homopolymeric IFs. The position of the cytotardin rod domain, containing the coiled-coil and linkers (coil 1A, L1, coil 1B, L12, coil 2; predicted from the protein sequence alignment in Figure 2), is indicated by blue lines. Note the sequence similarities of the rod domain, especially at the rod domain-flanking intermediate filament consensus motifs (highlighted in red). Note also 42 amino acids in the coil 1B of cytotardin, which have been deleted from the ancestral cytoplasmic IF protein gene in chordates. The alignment (Clustal Omega) has been performed using Analysis Tool Web Services from the EMBL-EBI (McWilliam et al. 2013, Nucleic Acids Res. 41, W597–W600). (*) indicates positions which have a single, fully conserved residue. (:) Indicates conservation between groups of strongly similar properties — scoring > 0.5 in the Gonnet PAM 250 matrix. (.) Indicates conservation between groups of weakly similar properties — scoring ≤ 0.5 in the Gonnet PAM 250 matrix.

Figure 2—figure supplement 2. Protein sequence alignment of *H. dujardini* IF proteins with selected IF proteins from *Caenorhabditis elegans*. *C. elegans* ifa-1 and ifb-1 are epithelial cytoplasmic intermediate filament proteins, whereas lmn-1 represents the single lamin of *C. elegans*. The position of the cytotardin rod

domain, containing the coiled-coil and linkers (coil 1A, L1, coil 1B, L12, coil 2; predicted from the protein sequence alignment in Figure 2), is indicated by blue lines. The intermediate filament consensus motifs are highlighted in red, the immunoglobulin fold (Ig fold) is marked in light orange, and the C-terminal prenylation motif of lamins (CaaX) is marked in purple. Note the presence of a prenylation motif in *H. dujardini* lamin-2 and *C. elegans* lmn-1 and its absence in the other proteins. The alignment (Clustal Omega) has been performed using Analysis Tool Web Services from the EMBL-EBI (McWilliam et al. 2013, Nucleic Acids Res. 41, W597–W600). (*) indicates positions which have a single, fully conserved residue. (:) Indicates conservation between groups of strongly similar properties — scoring > 0.5 in the Gonnet PAM 250 matrix. (.) Indicates conservation between groups of weakly similar properties — scoring ≤ 0.5 in the Gonnet PAM 250 matrix.

Figure 3—figure supplement 1. Maximum likelihood tree under a dataset-specific GTR+G substitution model and accession numbers of 447 eukaryotic intermediate filament proteins and the placement of the IF protein genes of the tardigrade *Hypsibius dujardini* (highlighted in red). Lamins of onychophorans are highlighted in orange, copepods in purple, collembolans in green, nematodes in light brown and cytoplasmic IF proteins of nematodes in dark brown. Note the position of isomin of the collembolan *Isotomurus maculatus*, which has been interpreted as a putative cytoplasmic IF protein (Mencarelli et al. 2011, BMC Biol. 9, 17), within a group of collembolan lamins (asterisk). The domain structure of each protein is depicted on the right. Note the absence of a

730 nuclear localization signal (NLS) in cytotardin of *H. dujardini* as well as in the
731 coloured sequences of copepods (purple) and collembolans (green). Bootstrap
732 values from 1,000 pseudoreplicates > 50% are given at the nodes. Scale bar
733 indicates the number of substitutions per site. Abbreviations: CaaX,
734 isoprenylation motif at the carboxyl terminus; LTD, lamin tail domain; NLS,
735 nuclear localization signal.
736
737 **Figure 3—figure supplement 2.** Maximum likelihood tree under the empirical
738 LG+G substitution model and accession numbers of 447 eukaryotic
739 intermediate filament proteins and the placement of the IF protein genes of the
740 tardigrade *Hypsibius dujardini* (highlighted in red). Lamins of onychophorans
741 are highlighted in orange, copepods in purple, collembolans in green,
742 nematodes in light brown and cytoplasmic IF proteins of nematodes in dark
743 brown. Note the position of isomin of the collembolan *Isotomurus maculatus*,
744 which has been interpreted as a putative cytoplasmic IF protein (Mencarelli et
745 al. 2011, BMC Biol. 9, 17), within a group of collembolan lamins (asterisk). The
746 domain structure of each protein is depicted on the right. Note the absence of a
747 nuclear localization signal (NLS) in cytotardin of *H. dujardini* as well as in the
748 coloured sequences of copepods (purple) and collembolans (green). Bootstrap
749 values from 1,000 pseudoreplicates > 50% are given at the nodes. Scale bar
750 indicates the number of substitutions per site. Abbreviations: CaaX,
751 isoprenylation motif at the carboxyl terminus; LTD, lamin tail domain; NLS,
752 nuclear localization signal.
753

754 **Figure 4—figure supplement 1.** Western blots of lamin-1, lamin-2 and
755 cytotardin antisera. (**A**) Western blot analysis of lamin-1 protein expression in *H.*
756 *dujardini*. Anti-lamin-1 antibody stains a band of ≈70 kDa, as expected. (**B**)
757 Western blot analysis of lamin-2 protein expression in *H. dujardini*. Anti-lamin-2
758 antibody stains a band of ≈72 kDa, as expected. (**C**) Western blot analysis of
759 cytotardin protein expression in *H. dujardini*, transformed *E. coli* and transfected
760 MCF-7 cells. Anti-cytotardin antibody stains a band of ≈57 kDa, as expected.
761
762 **Figure 4—figure supplement 2.** Immunofluorescence labelling of lamin-1 and
763 lamin-2 in the tardigrade *Hypsibius dujardini*. Confocal laser-scanning
764 micrographs. Sagittal sections of specimens. Anterior is left, dorsal is up. Note
765 the presence of lamin-1 and lamin-2 inside all nuclei. Cuticular structures of the
766 foregut are autofluorescent. (**A, B**) Double labelling of lamin-1 (glow-mode) and
767 DNA (cyan) on a cryosection. (**C, D**) Double labelling of lamin-2 (glow-mode)
768 and DNA (cyan) on a cryosection. br, position of the brain; bt, buccal tube; cg,
769 claw gland; lg1–lg4, legs 1 to 4; mi, position of the midgut; nu, nuclei; ov, ovary;
770 ph, pharynx; sg, salivary gland. Scale bars: (**A–D**) 10 µm.
771
772 **Figure 4—figure supplement 3.** Immunofluorescence labelling of cytotardin in
773 the tardigrade *Hypsibius dujardini* with focus on the epidermis. Confocal laser-
774 scanning micrographs. (**A**) Double labelling of cytotardin (glow-mode) and DNA
775 (cyan) on a cryosection. Sagittal section of a specimen. Anterior is left, dorsal is
776 up. Note the exclusive presence of cytotardin filaments in the epidermis and
777 tissues of the foregut. (**B**) Anti-cytotardin immunolabelling on a cryosection.

Tangential section of dorsolateral body wall. Arrows point to the dorsal midline. (**C, D**) Double labelling of cytotardin (glow-mode) and DNA (cyan) on a whole-mount preparation of a contracted specimen. Detail of the third pair of legs in ventral view. Anterior is up. Note the apical position of cytotardin-filament belts in the epidermal cells (arrowheads) and their dense arrangement in the tips of each leg. br, brain; bt, buccal tube; cg, claw gland; cl, claw; ep, epidermis; lg, leg; lg1–lg4, legs 1 to 4; mc, mouth cone; mi, position of the midgut; nu, nuclei; oe, oesophagus; ov, ovary; ph, pharynx. Scale bars: (**A–D**) 10 µm.

Figure 5—figure supplement 1. Characterization of cytotardin antiserum. (**A–C**) Triple labelling of cytotardin (glow-mode), HA-tag (green) and DNA (cyan) in MCF-7 cells transfected with pcDNA3-HA-cytotardin plasmids. Anti-cytotardin and anti-HA-tag staining show similar signals confirming the specificity of anti-cytotardin antibodies. HA-cytotardin is cytoplasmic and forms short filaments able to localize close to cell borders. (**D**) Western blot analysis of cytotardin in MCF-7 cells transfected with pcDNA3-cytotardin, pcDNA3-HA-cytotardin, pEGFP-cytotardin and the corresponding empty vectors. Left panel shows a Ponceau red-staining of the blotted cell extract as loading control. Anti-tag (right panel) compared to anti-cytotardin (middle panel) staining shows the expression of the exogenous protein and specificity of the antibodies for immunoblotting. nu, nucleus. Scale bars: (**A–C**) 10 µm.

Figure 5—figure supplement 2. Plasmids, primers, and restriction enzymes used for the cloning of tardigrade lamins and cytotardin.

Figure 6—figure supplement 1. Immunofluorescence labelling of cytotardin in the tardigrade *Hypsibius dujardini* with focus on the foregut. Confocal laser-scanning micrographs. Double labelling of cytotardin (glow-mode) and DNA (cyan) on sagittal (**A–C, E**) and cross sections (**D**) of cryosectioned specimens. Cuticular structures of the foregut are autofluorescent. Anterior is left (**A–C, E**); dorsal is up (in **A–E**). (**A**) Overview of the foregut. Note the dense arrangement of cytotardin arrays in the epithelia of the foregut, especially those surrounding the stylets. (**B**) Detail of the buccal tube. (**C**) Detail of the pharynx. (**D**) Cross-section of the pharynx. (**E**) Detail of the oesophagus. bt, buccal tube; mc, mouth cone; nu, nucleus; oe, oesophagus; pc, placoid; ph, pharynx; pm, pharyngeal myoepithelium; st, epithelium surrounding the stylets. Scale bars: (**A–E**) 5 µm.

Videos

Video 1. The tardigrade *Hypsibius dujardini* survives freezing. This time-lapse video shows thawing specimens of the tardigrade *H. dujardini* after 4 days frozen in ice. One specimen starts with minuscule movements of one leg after 20 minutes of thawing and fully recovers locomotion within 120 minutes.

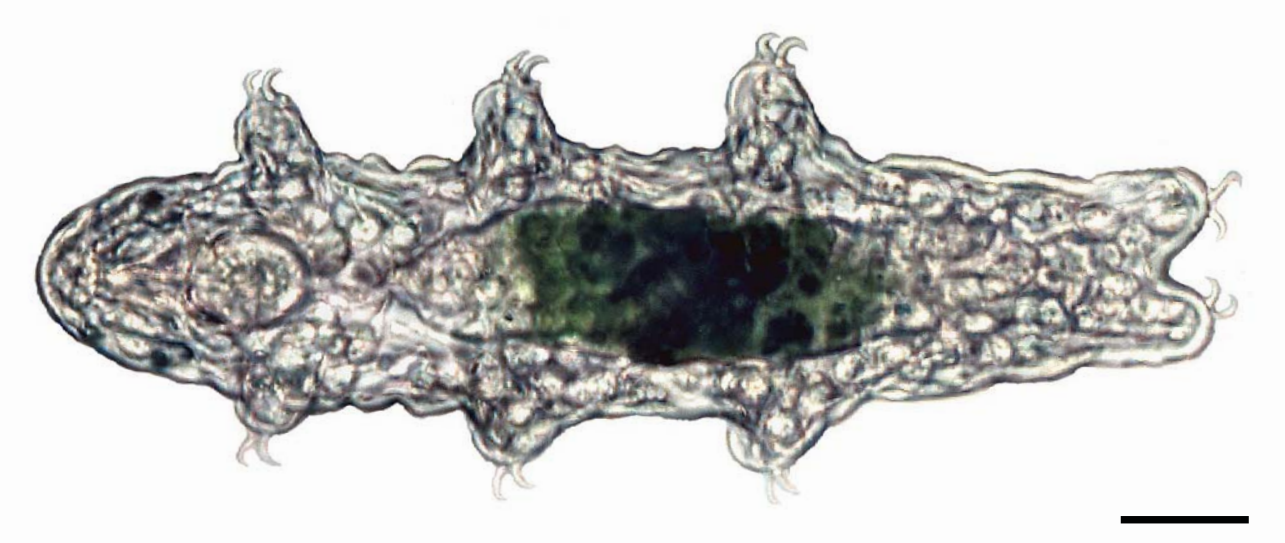

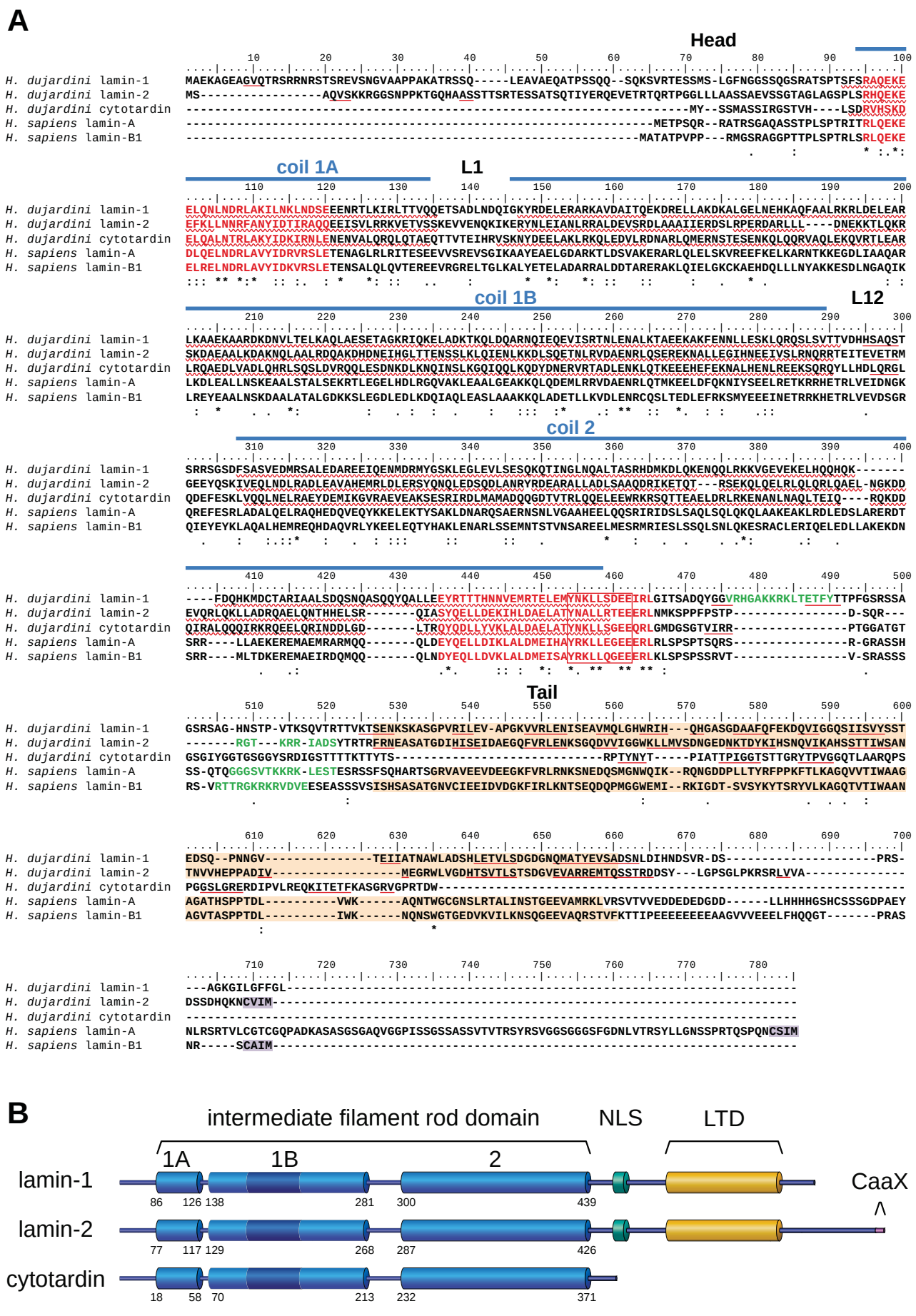
A
Head
coil 1A
L1
coil 1B
L12
coil 2
Tail
H. dujardini lamin-1
H. dujardini lamin-2
H. dujardini cytotardin
H. sapiens lamin-A
H. sapiens lamin-B1
B
intermediate filament rod domain
NLS
LTD
1A
1B
2
lamin-1
lamin-2
cytotardin
CaaX
86 126 138 281 300 439
77 117 129 268 287 426
18 58 70 213 232 371

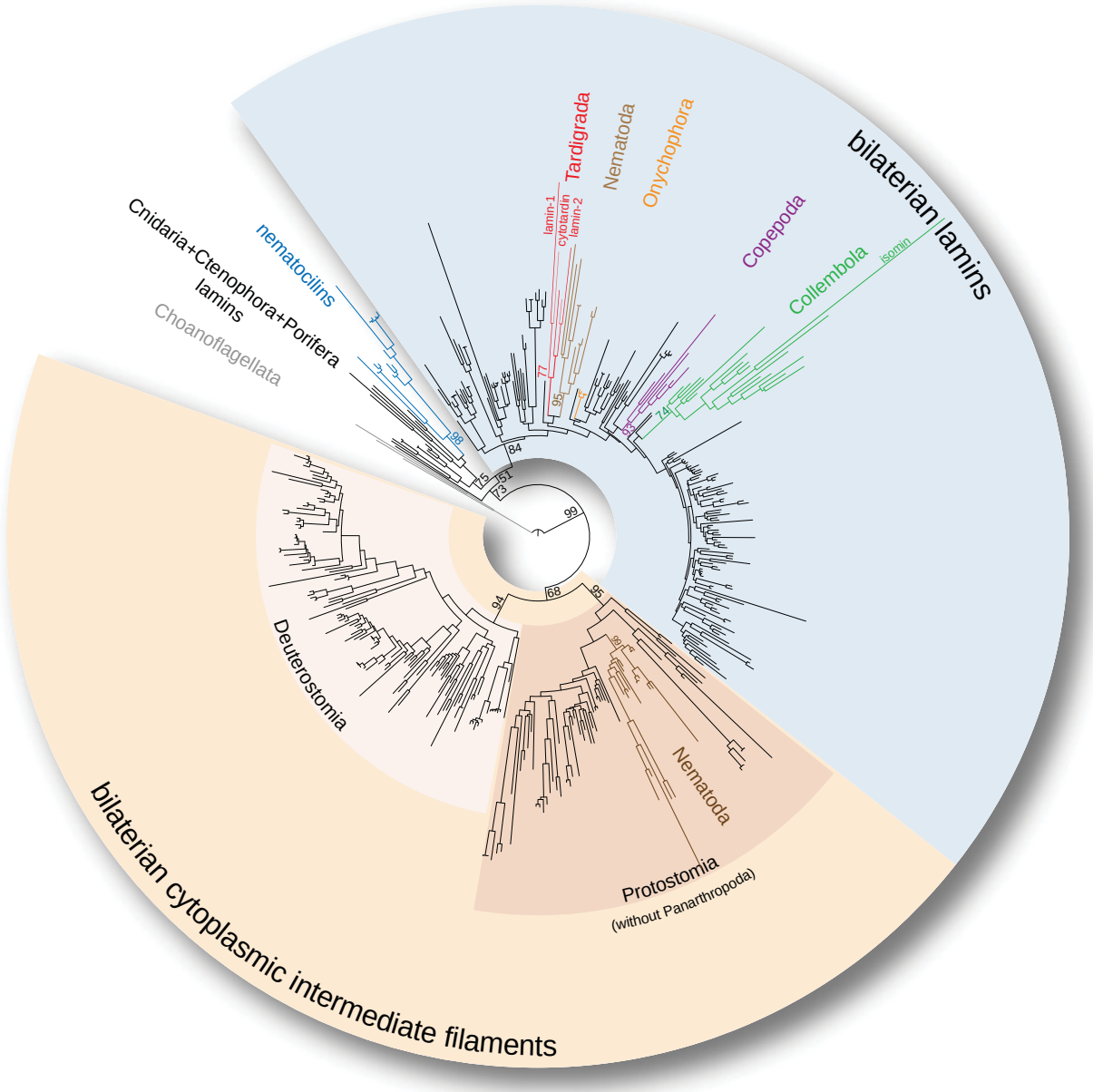
bilaterian lamins
Tardigrada
Nematoda
Onychophora
Copepoda
Collembola
Isomin
lamin-1
cytoplasmic lamin-2
nematocilins
Cnidaria+Ctenophora+Porifera lamins
Choanoflagellata
bilaterian cytoplasmic intermediate filaments
Deuterostomia
Nematoda
Protostomia
(without Panarthropoda)

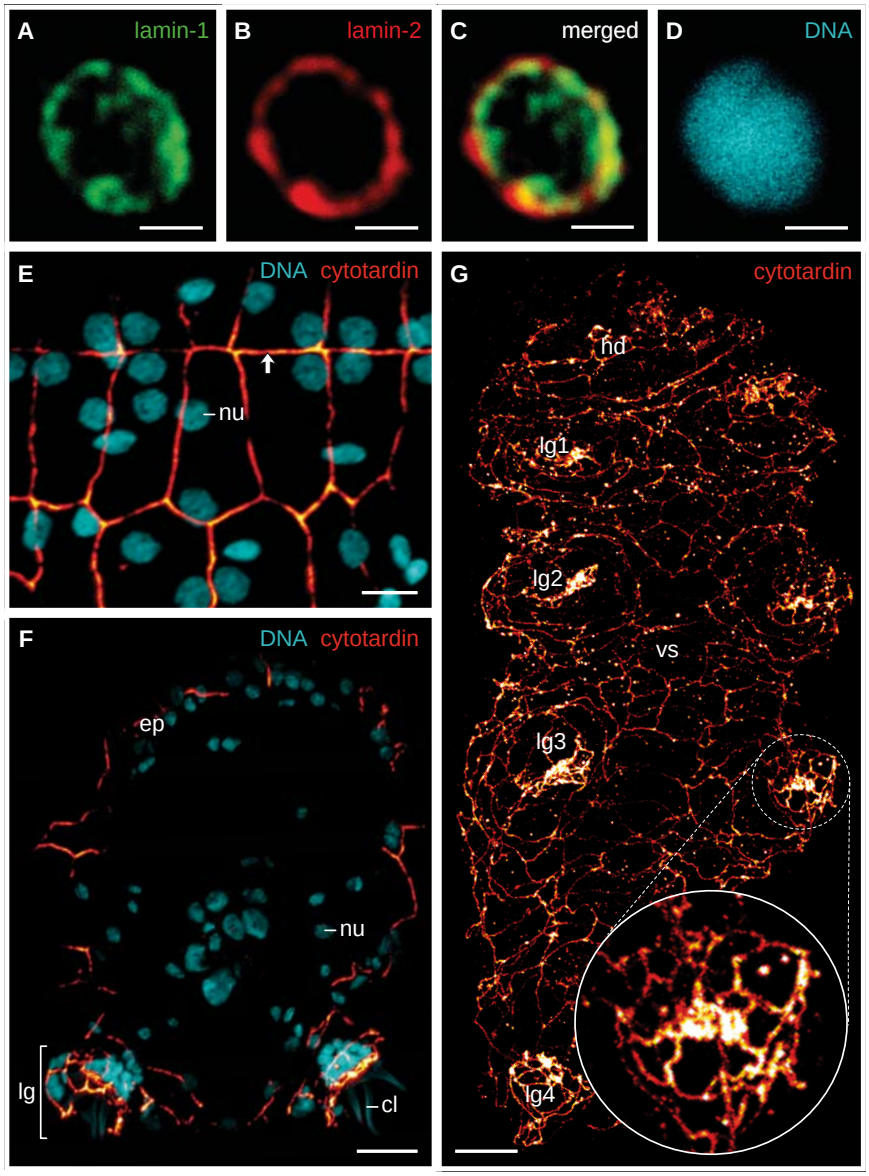
A
lamin-1
B
lamin-2
C
merged
D
DNA
E
DNA cytotardin
nu
F
DNA cytotardin
ep
nu
lg
cl
G
cytotardin
hd
lg1
lg2
vs
lg3
lg4